

A Profust Reliability Based Approach to Prognostics and Health Management

Zhiyao Zhao, Quan Quan, and Kai-Yuan Cai

Abstract—Prognostics and health management (PHM) technology has been widely accepted, and employed to evaluate system performance. In practice, system performance often varies continually rather than just being functional or failed, especially for a complex system. Profust reliability theory extends the traditional binary state space $\{0, 1\}$ into a fuzzy state space $[0, 1]$, which is therefore suitable to characterize a gradual physical degradation. Moreover, in profust reliability theory, fuzzy state transitions can also help to describe the health evolution of a component or a system. Accordingly, this paper proposes a profust reliability based PHM approach, where the profust reliability is employed as a health indicator to evaluate the real-time system performance. On the basis of the health estimation, the system remaining useful life (RUL) is further defined, and the mean RUL estimate is predicted by using a degraded Markov model. Finally, an experimental case study of Li-ion batteries is presented to demonstrate the effectiveness of the proposed approach.

Index Terms—Prognostics and health management, profust reliability, health estimation, remaining useful life.

ACRONYMS AND ABBREVIATIONS

PHM	Prognostics and health management
RUL	Remaining useful life
RCC	Remaining charge cycles

NOTATION

x	Continuous system state
$\mu_S(x)$	Membership function of fuzzy success state
$\mu_F(x)$	Membership function of fuzzy failure state
m_{xy}	Transition from state x to state y
$\mu_{TSF}(m_{xy})$	Membership function of transition from fuzzy success state to fuzzy failure state
$p_{xy}(t_0, t)$	Transition probability from state x to state y
$P(t_0, t)$	Transition probability matrix

Manuscript received January 20, 2013; revised July 23, 2013; accepted October 13, 2013. Date of publication January 16, 2014; date of current version February 27, 2014. This work was supported by the National Natural Science Foundation of China under Grants 61104012, 51375462, and 61272164, the 973 Program under Grant 2010CB327904, and the Ph.D. Programs Foundation of Ministry of Education of China under Grant 20111102120008. Associate Editor: Z. Li

The authors are with School of Automation Science and Electrical Engineering, Beihang University, Beijing 100191, China (e-mail: zzy@asec.buaa.edu.cn; qq_buaa@buaa.edu.cn; kycai@buaa.edu.cn).

Color versions of one or more of the figures in this paper are available online at <http://ieeexplore.ieee.org>.

Digital Object Identifier 10.1109/TR.2014.2299111

$\phi_x(t)$	State probability of state x
$\Phi(t)$	State probability vector
$R(t_0, t)$	Profust interval reliability
$R(t)$	Profust reliability
F_T	Failure threshold
$r(t)$	Remaining useful life
S_i	Discrete system state
$W(t)$	Estimation window
T	Sample time
Δ	Length of estimation window, $\Delta = kT, k \in \mathbb{N}^+$
Γ	Profust reliability trajectory
λ	Degradation factor
C	Charge cycle
r_c	Remaining charge cycles

I. INTRODUCTION

PROGNOSTICS AND HEALTH MANAGEMENT (PHM) is defined as an approach utilizing measurements, models, and software to perform incipient fault detection, condition assessment, and failure progression prediction [1]. As shown in Fig. 1, an integrated PHM framework generally incorporates functions of data processing, condition monitoring & health estimation, remaining useful life (RUL) prediction, and condition-based maintenance (CBM) & intelligent decision-making [2]. Currently, the existing PHM approaches have already covered each part of the PHM system for various types of vehicles, systems, and products. In terms of the usage of information, these approaches can be classified into three types [3]: the physics-of-failure (PoF) approach, the data-driven approach, and the fusion approach.

1) *The PoF Approach*: The PoF approach takes the knowledge of a product's lifecycle loading conditions into consideration, together with the failure modes, mechanisms, and sites to perform reliability modeling and assessment [4]. The PoF approach was commonly employed in the PHM of various electronic products [5]–[10]. Pecht introduced an integrated framework of a PoF-based PHM approach for electric products, and presented a unified implementation including failure modes, mechanisms, and effects analysis (FMMEA), data reduction, and feature extraction [11]. PoF models were also employed in the RUL prediction of mechanical products such as aircraft engine bearings [12], and flight control actuators

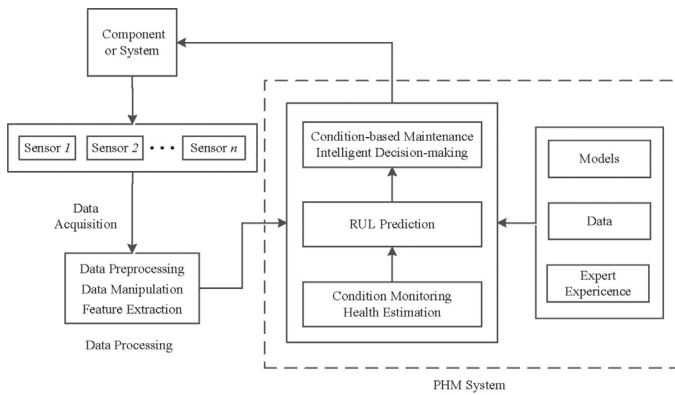


Fig. 1. PHM framework.

[13]. The main advantage of the PoF approach is the available physical understanding and known failure mechanisms of components or products, which is able to obtain high accuracy of the prognostics. However, most PoF approaches mainly focus on the component level, because it is often difficult, costly, or even impossible to accurately model the complex physical degradation of a system containing large numbers of subsystems and components. This situation may to some extent limit their engineering applications.

2) *The Data-Driven Approach*: The data-driven approach uses mathematical analysis of current and historical data to provide signals of abnormal behavior, and estimate RUL [11]. The neural network is the most popular technique in data-driven approaches [14], which has been applied to the PHM activities of gearboxes [15], bearings [16], [17], chiller systems [18], aircraft actuators [19], and Gas Turbines [20]. Other techniques such as the relevance vector machine (RVM) [21], the hidden Markov model (HMM) [22], [23], and the Bayesian network [24] were also employed in data-driven approaches. The competitive advantage of the data-driven approach is that the system behavior can be learned only from monitored data with less system model knowledge, which is less complex and more applicable than the PoF approach. However, the drawback includes a potentially long learning time, and a lack of sufficient training data in practice, especially for non-operating systems. In terms of precision, the data-driven approach gives less precise results than the PoF one.

3) *The Fusion Approach*: The fusion approach combines PoF and data-driven models for PHM, overcoming some drawbacks of using either approach alone [25]. For example, in [26], a fusion approach was implemented to assess and mitigate reliability risks arising from free air cooling in a data center. FMMEA was conducted to identify the weakest subsystems or components, and was able to identify the critical failure mechanisms and key parameters which indicated the degradation trends of the system. Further, the data-driven approach identified the failure precursor parameters, which were indicative of impending failures based on system performance and the collected data. Other interesting works related to fusion approaches can be found in [27]–[29].

From the aforementioned approaches, compared with PoF approaches, it is easy to see that data-driven approaches are

more suitable for a complex system because the system model is difficult to obtain [3]. However, most existing data-driven approaches focus on either a specific system component, or a general PHM framework. Moreover, the approaches often rely on a comparison between in-situ parameters and healthy baselines to detect system anomalies, and evaluate system performance, which is difficult to describe the whole system physical degradation.

For such a purpose, this paper aims to propose a unified theoretical foundation for PHM based on profust reliability theory [30], [31]. Compared with traditional reliability theory, profust reliability theory is more suitable for PHM. Traditional reliability approaches are always based on the analysis of historical life-test data, which yield statistical results only reflecting population characteristics of the same kind of systems under typical conditions. However, PHM is related to on line system reliability characteristics that are strongly affected by applications and operating conditions in practice. Moreover, variations also exist among individual systems. Thus, traditional reliability approaches, although widely used, have limitations in estimating reliability for individual systems under dynamic operating and environmental conditions [32]. In contrast, as a part of fuzzy reliability theory [30], [31], [33]–[36], profust reliability theory extends the traditional binary state space $\{0, 1\}$ into a fuzzy state space $[0, 1]$, and models fuzzy state transitions for a component or system representing various degrees of success and failure. This feature enables a profust reliability based approach to track real-time operational performance, and characterize the physical degradation and property evolution of a specific system. Furthermore, a complex system can work at a degraded level, and the performance is always described by fuzzy measurements. Therefore, the profust reliability based approach is a potential method for PHM of complex systems.

This paper integrates PHM with profust reliability theory, which distinguishes from a recent paper of ours presented at PHM2013 (2013 Prognostics and System Health Management Conference) [37]. In the work presented in [37], based on profust reliability theory, an algorithm in a discrete time domain was proposed to measure the health of a class of Li-ion batteries with data downloaded from the NASA website [38]. Moreover, the health status was classified into different levels according to the corresponding profust reliability. Compared with [37], a generalized approach including a comprehensive case study is presented in this paper. As a result, there are significant differences between the work presented in this paper and that presented in [37]. i) A profust reliability based PHM approach is developed, which involves the continuous time domain as well as the discrete time domain, whereas the algorithm presented in [37] is confined to the discrete time domain. ii) The system studied in this paper is distinguished from that in [37]. The approach proposed in this paper is to describe the health of a complex system with multi-parameters and multi-components, whereas the algorithm proposed in [37] is devoted to systems with a single parameter. iii) An important, new contribution, namely the system RUL prediction algorithm, which is not contained in [37], is developed based on the health estimation results. Accordingly, the experiments on RUL prediction of these Li-ion batteries are further performed and discussed.

The paper makes three major contributions. First, this paper proposes an alternative data-driven PHM approach. With the system-level integration between PHM and profust reliability theory, it offers a theoretical support to the PHM of complex systems. Second, the system binary states (either functional or failed) are extended to fuzzy states, and transitions among them are employed to evaluate system performance based on profust reliability theory. Finally, the proposed profust reliability is developed as a unified health indicator for different kinds of systems, which differs among most existing data-driven approaches only relying on various system parameters.

The remainder of this paper is organized as follows. Section II proposes a methodology framework of the PHM approach based on profust reliability theory, including a health estimation module, and a RUL prediction module. Section III presents an implementation process of the proposed approach. In Section IV, a case study of Li-ion batteries is employed to validate the proposed approach, and the experimental results are given and discussed. Finally, Section V gives a conclusion, and indicates the limitation and future development of the proposed approach.

II. METHODOLOGY FRAMEWORK

Let $U = \{x \mid a \leq x \leq b\}$ be a continuous domain. In the domain U , system fuzzy success states are defined as

$$S = \{x, \mu_S(x); x \in U\}, \quad (1)$$

and fuzzy failure states are defined as

$$F = \{x, \mu_F(x); x \in U\}. \quad (2)$$

Under the fuzzy state assumption, the operational states of parameters characterizing a component or a complex system can be described with the degree of fuzzy health membership, rather than just successful and failed states, through single threshold segmentation. In general, we have

$$\mu_S(x) = 1 - \mu_F(x), x \in U. \quad (3)$$

Profust reliability theory models fuzzy state transitions for a component or system representing various degrees of success and failure. Here, assume the fuzzy state transitions possess the Markov property.

Assumption 1: Let the stochastic process $X = \{X(t), t \geq 0\}$ represent a sequence of system states with time. If $P\{X(t_0) =$

$x_0, X(t_1) = x_1, \dots, X(t_n) = x_n\} > 0$, then the transition probability satisfies that [see (4) at the bottom of the page]. $\forall t, 0 \leq t_0 \leq t_1 \leq \dots \leq t_n, x_k \in U, 0 \leq k \leq n, n \in \mathbb{N}^+$.

Remark 1: *Assumption 1* indicates that the system state at time t_n only depends on the system state at time t_{n-1} . It is reasonable to use a Markov process to model system state transitions, when the lifecycle of the studied system conforms to a negative exponential distribution, namely the system has the memoryless property.

Definition 1: Let $U_T = \{m_{xy} \mid x \in U, y \in U\}$. In the domain U_T , a transition from a fuzzy success state to a fuzzy failure state is defined as [30]

$$T_{SF} = \{m_{xy}, \mu_{T_{SF}}(m_{xy}); x, y \in U\}, \quad (5)$$

where T_{SF} is viewed as a fuzzy event, and the corresponding membership function $\mu_{T_{SF}}(m_{xy})$ is determined as [30]

$$\mu_{T_{SF}}(m_{xy}) = \begin{cases} \beta_{F|S}(y) - \beta_{F|S}(x) & \text{if } \beta_{F|S}(y) > \beta_{F|S}(x) \\ 0 & \text{otherwise} \end{cases} \quad (6)$$

$$\beta_{F|S}(x) = \frac{\mu_F(x)}{\mu_S(x) + \mu_F(x)}, x \in U. \quad (7)$$

Remark 2: Here, $\beta_{F|S}(x)$ is interpreted as the weight that state x is attached to the fuzzy failure state compared with the fuzzy success state. In this case, only if condition $\beta_{F|S}(y) > \beta_{F|S}(x)$ is true, a transition from state x to state y promotes the transition from fuzzy success to fuzzy failure.

Definition 2: Let $A = \{T_{SF} \text{ does not occur during a time interval } [t_0, t]\}$. For $x, y \in U$, the profust interval reliability over the time interval $[t_0, t]$ is defined as (8) at the bottom of the page [30].

The profust reliability is defined as [30].

$$R(t) = R(0, t). \quad (9)$$

Remark 3: The system's reliability is decreasing during its use because of the components' degradation. Thus, the profust reliability is closely related to the system performance, and therefore served as a natural indicator of the system health status. However, it is difficult to calculate the profust reliability $R(t)$ by (9) in practice. Also, it is inappropriate to perform (8) in real-time performance monitoring, because it only concentrates on system degradation during the time interval $[t_0, t]$ without considering the system health status at time t_0 . For the

$$\begin{aligned} & P\{X(t_n) = x_n \mid X(t_0) = x_0, X(t_1) = x_1, \dots, X(t_{n-1}) = x_{n-1}\} \\ & = P\{X(t_n) = x_n \mid X(t_{n-1}) = x_{n-1}\} \end{aligned} \quad (4)$$

$$R(t_0, t) = P(A) = 1 - P(\bar{A}) = 1 - \int_a^b \int_a^b \mu_{T_{SF}}(m_{xy}) dp_{xy}(t_0, t). \quad (8)$$

purpose of real-time performance monitoring, the concept of conditional reliability is extended to real-time applications in [32]. Similarly, a novel algorithm of $R(t)$ is proposed here.

Definition 3: Let $B = \{\text{The system is in a fuzzy success state at a time } t_0\}$. For $x, y \in U$, and a time interval $[t_0, t]$, the profust reliability $R(t)$ is computed as (10) at the bottom of the page. The time interval $[t_0, t]$ can be viewed as an estimation interval.

Remark 4: Equation (10) denotes that the profust reliability $R(t)$ is computed by using information including the system performance at the initial time t_0 , and state transitions during the time interval $[t_0, t]$. The physical meaning of profust reliability $R(t)$ is that, after a specific time t_0 , no further substantial performance deterioration occurs during the time interval $[t_0, t]$. The value of $R(t)$ belongs to $[0, 1]$. The situation of $R(t) = 1$ means that the system is in a fully successful state, while $R(t) = 0$ means that the system has completely failed. Without maintenance actions, $R(t)$ is a monotonically non-increasing function under ideal conditions. However, in practice, observation noise, system noise, and external disturbance will cause fluctuations of $R(t)$ in a small range.

Remark 5: Note that t_0 and t are usually not restricted to adjacent time indexes in (10). This means $p_{xy}(t_0, t)$ is a k -step transition probability, provided that $t - t_0 = kT$, where T is the sample time, $k \in \mathbb{N}^+$, $k \neq 1$.

The status of human health can be divided into different levels such as health, sub-health, disease, and serious illness. Also, the severity degree of meteorological disasters is described with levels, mainly because a qualitative index is easy to be understood by non-technical users. Inspired by that approach, we propose the concept of system health level in terms of the continuous health indicator $R(t)$, is shown in (11) at the bottom of the page, where a_1, a_2, \dots, a_{n-1} represent the classification thresholds.

Remark 6: The establishment of health levels is mainly applied to the management phase in the PHM framework, such as the maintenance schedule and resource management in CBM, which is beyond the scope of this paper. From another perspective, the health level can improve the robustness, and partly mitigate the sensitivity of health estimation results to disturbances caused by fluctuations of $R(t)$. Here, the level numbers and thresholds among adjacent levels are usually determined based

on information of similar systems, and the engineers' understanding to system performance, which can affect the selection of the optimal maintenance policy. Actually, the introduction of health levels is not a compulsive step in the proposed PHM approach, because the value of the profust reliability is capable of evaluating system performance. The existence of this step depends on the requirement of practical engineering applications.

On the basis of the health estimation¹, a RUL definition based on the profust reliability is proposed here referring to [39].

Definition 4: Let F_T be the system failure threshold. The RUL at a time t_i is defined as

$$r(t_i) = t_j - t_i, \text{ where } t_j = \max_t \{R(t) \geq F_T\}. \quad (12)$$

Remark 7: The true RUL of a system is obtained only if the system is completely failed, or deemed as unusable. Thus, for an incompletely failed system in operation, the RUL can only be estimated with system operational information up to the current time.

Definition 5: As shown in Fig. 2, let $\hat{\Gamma}(t_i)$ be the trajectory of a predicted profust reliability sequence from time t_i such that $\hat{\Gamma}(t_i) = \{R(t_i), \hat{R}(t_{i+\Delta} | t_i), \dots, \hat{R}(t_{EoP} | t_i); \Delta = kT, k \in \mathbb{N}^+\}$, where T is the sample time, and t_{EoP} is the time when the prediction ends. Let $\hat{r}(t_i)$ be the estimate of the RUL at the current time t_i , and F_T be the system failure threshold. Then, the mean value of the RUL estimate is defined as

$$\hat{r}(t_i) = t_j - t_i, \text{ where } t_j = \max_t \{\hat{R}(t | t_i) \geq F_T\}. \quad (13)$$

Remark 8: The estimate of RUL is obtained based on the prediction of profust reliability variation after system performance deteriorates or a fault is detected. Note that the prediction of the profust reliability variation trajectory is achieved till the predicted profust reliability curve reaches the predetermined F_T . The system failure threshold F_T can be developed based on engineers' understanding of system performance. Generally, there is useful information available to help select appropriate failure thresholds such as historical data, and information of similar cases.

¹The presented health estimation work is an extension of Section 3.1 in [37].

$$\begin{aligned} R(t) &= P(A | B) \cdot P(B) \\ &= 1 - P(\bar{A} | B) \cdot P(B) - P(\bar{B}) \\ &= 1 - \int_a^b \int_a^b \mu_{T_{SF}}(m_{xy}) dp_{xy}(t_0, t) \cdot \int_a^b \mu_S(x) d\phi_x(t_0) - \int_a^b \mu_F(x) d\phi_x(t_0) \end{aligned} \quad (10)$$

$$\text{System Health Level} = \begin{cases} \text{Health Level-1} & R(t) \in [0, a_1) \\ \text{Health Level-2} & R(t) \in [a_1, a_2) \\ \dots & \dots \\ \text{Health Level-n} & R(t) \in [a_{n-1}, 1] \end{cases} \quad (11)$$

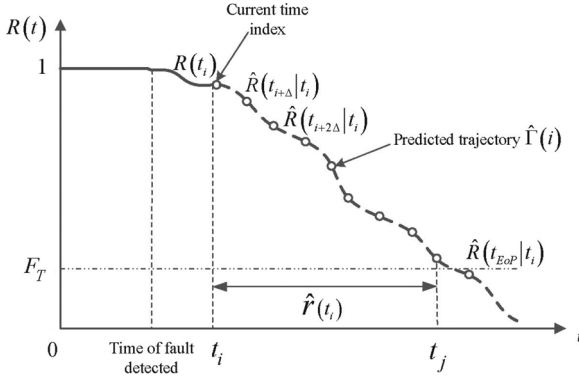


Fig. 2. A profust reliability trajectory prediction and RUL estimate.

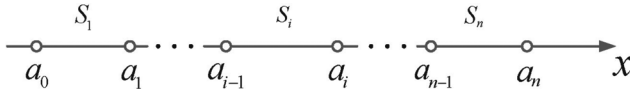


Fig. 3. Discretization diagram.

III. IMPLEMENTATION PROCESS

Profust reliability $R(t)$ plays a core role in the implementation of the proposed approach. After obtaining $R(t)$, the proposed RUL in *Definition 5* can be predicted based on the health estimation results. In this section, the implementation process of the proposed methodology is presented in the following four steps below.

A. Discretization

To calculate $R(t)$ by *Definition 3*, the transition probability $p_{xy}(t_0, t)$, the system state probability $\phi_x(t_0)$, and the corresponding membership functions are required. Traditional reliability methods relying on the collection of failure data can be employed to get the probability distribution function of $p_{xy}(t_0, t)$ and $\phi_x(t_0)$ in a continuous domain. However, these methods assume that the operating conditions and the failure mechanism of the complex system in practical engineering applications are well addressed in reliability tests, which is hard to satisfy [26]. In this case, it is inappropriate to calculate $p_{xy}(t_0, t)$ and $\phi_x(t_0)$ by imprecise probability distribution functions. In the proposed approach, the continuous domain U is firstly discretized, and $p_{xy}(t_0, t)$ and $\phi_x(t_0)$ are further calculated in a discretized domain by the statistical method.

Theorem 1: For $U = \{x \mid a \leq x \leq b\}$, let $S_i = \{x \mid a_{i-1} \leq x \leq a_i\}$ as shown in Fig. 3, where $\delta = \frac{b-a}{n}$, $a_i = a + i \cdot \delta$, $i = 1, 2, \dots, n$. Then, $R(t)$ in *Definition 3* is (14) at the bottom of the page.

Proof: See the Appendix.

Remark 9: In *Theorem 1*, n determines the degree of discretization. Theoretically, $R(t)$ in *Theorem 1* will be infinitely

close to $R(t)$ in *Definition 3* if n approaches infinity. However, a large n will lead to heavy calculations which may not satisfy the needs of real-time condition monitoring. On the other hand, a small n will affect PHM sensitivity because of insufficient fuzzification. Thus, the value n needs to be appropriately selected in practical engineering applications.

Remark 10: The definition of membership functions plays an important role in calculating $R(t)$ by *Theorem 1*, because an inappropriate membership function will lead to problems such as false detection of anomalies, and failure to detect anomalies. First, for a single parameter, the function type needs to be selected based on the system parameter type, and practical engineering requirements. For example, when a system is working in a fully successful state, a triangular or trapezoidal membership function [40] should be chosen if a parameter is required to stay at a fixed value or a range, respectively. Second, the thresholds of a membership function can be determined by reference range provided by the data sheet, historical data, and information of similar products or systems. For a complex system containing multi-parameters and multi-components, the membership calculation is shown in the Appendix.

B. Transition Probability, and State Probability Calculation

Let $P(t_0, t) = [p_{ij}(t_0, t)]_{n \times n} \in R^{n \times n}$ be the transition probability matrix of system states over the time interval $[t_0, t]$. The transition probability $p_{ij}(t_0, t)$ represents the probability of the transition from state S_i to state S_j over the time interval $[t_0, t]$, satisfying that

$$\begin{cases} p_{ij}(t_0, t) \geq 0 & 1 \leq i, j \leq n \\ \sum_{j=1}^n p_{ij}(t_0, t) = 1 & 1 \leq i \leq n \end{cases} \quad (15)$$

Then, the transition probability can be obtained by the statistical method [37]

$$p_{ij}(t_0, t) = \frac{n_{ij}(t_0, t)}{\sum_{j=1}^n n_{ij}(t_0, t)}, \quad (16)$$

where $n_{ij}(t_0, t)$ represents the number of transitions from state S_i to state S_j over the time interval $[t_0, t]$.

Remark 11: Equation (16) is true only if the law of large numbers [41] is satisfied, which requires a sufficiently long time interval $[t_0, t]$. Thus, adjacent time indexes are not selected as t_0 and t in *Definition 3*, which means $p_{xy}(t_0, t)$ is a multi-step transition probability as mentioned in *Remark 5*.

Let $\Phi(t)$ be the system state probability vector at time t ,

$$\Phi(t) = (\phi_{S_1}(t), \phi_{S_2}(t), \dots, \phi_{S_n}(t))^T \in R^{n \times 1}, \quad (17)$$

$$R(t) = 1 - \lim_{n \rightarrow \infty} \left\{ \left[\sum_{i=1}^n \sum_{j=1}^n \mu_{T_{SF}}(m_{ij}) \cdot p_{ij}(t_0, t) \right] \cdot \left[\sum_{i=1}^n \mu_S(S_i) \cdot \phi_{S_i}(t_0) \right] - \sum_{i=1}^n \mu_F(S_i) \cdot \phi_{S_i}(t_0) \right\} \quad (14)$$

where $\phi_{S_i}(t) (i = 1, 2, \dots, n)$ represents the state probability of system state S_i at time t . Then, we have

$$\Phi(t) = P(t_0, t) \cdot \Phi(t_0) \quad (18)$$

where $\Phi(t_0)$ is obtained iteratively using former time intervals. Assume that the state S_1 is the fully successful state. Then, before the system starts to work, we have

$$\Phi(0) = (1, 0, \dots, 0)^T. \quad (19)$$

C. Health Estimation

Following the two steps above, the real-time profust reliability $R(t)$ can be calculated using on-line data by applying *Theorem 1*. Here, real-time health estimation is implemented using two types of moving estimation windows. As shown in Fig. 4, $W(t)$ represents the Δ length estimation window at time t , which can be employed as the time interval presented in *Theorem 1*, $\Delta = kT$ (T is the sample time, $k \in \mathbb{N}^+$). The estimation window shown in Fig. 4(a) moves per sample time. This window can be used to obtain the profust reliability at each sample time such that

$$\Gamma_1 = \{\dots, R(t_i), R(t_i + T), R(t_i + 2T), R(t_i + 3T), \dots\}. \quad (20)$$

Similarly, Fig. 4(b) shows the type of moving per Δ length, which obtains the profust reliability at a fixed time interval Δ such that

$$\Gamma_2 = \{\dots, R(t_i), R(t_i + \Delta), R(t_i + 2\Delta), R(t_i + 3\Delta), \dots\}. \quad (21)$$

Remark 12: The length Δ of the proposed estimation window should be selected by considering both the law of large numbers mentioned in *Remark 11*, and the sensitivity of health estimation, because a large data volume could cover anomaly features, especially when a fault just appears. Thus, a balance should be sought according to practical applications.

Remark 13: In the process of health estimation, the movement of the estimation window in Fig. 4(a) has a higher estimation frequency than that in Fig. 4(b). Correspondingly, the whole estimation process is more time-consuming. Actually, Γ_2 can be viewed as a sampling of Γ_1 .

D. RUL Prediction

The key to predict RUL is to obtain a predicted profust reliability trajectory $\hat{\Gamma}(t)$ in *Definition 5*. According to *Assumption*

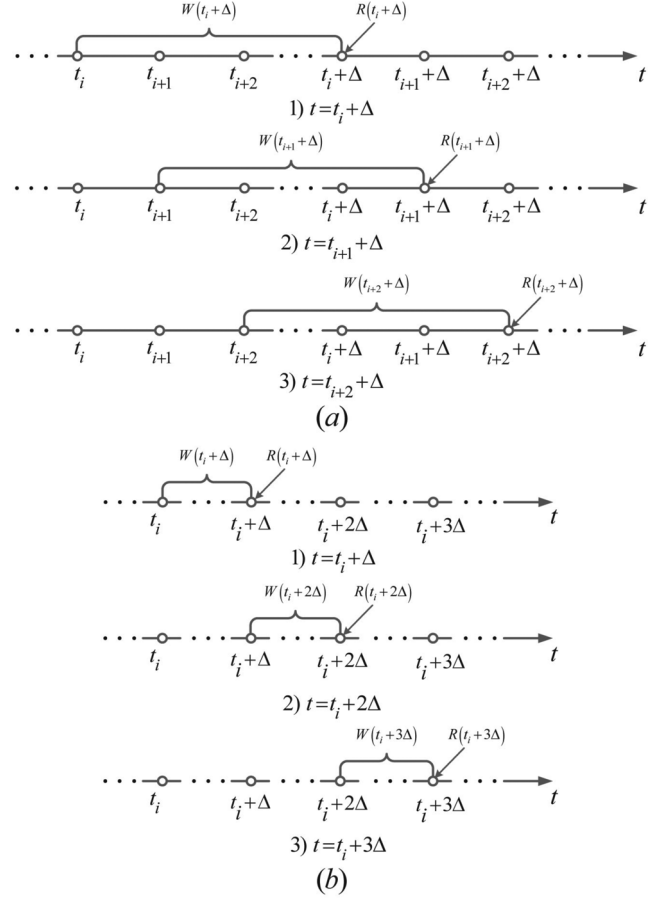


Fig. 4. Estimation window: (a) move per sample time, (b) move per window length.

I, the variation of the system health state is viewed as a Markov process. Note that this Markov process is non-homogeneous because a system tends to gradually become worn, and their health states become worse, as it grows older, namely the probability of becoming unhealthier will increase. This property leads to an imprecise estimate of profust reliability $\hat{R}(t + \Delta | t)$ by the transition probability matrix $P(t - \Delta, t)$. Therefore, a degraded Markov model is proposed here to calculate the estimate of profust reliability at a future time.

Lemma 1: Let $\lambda(t)$ be a degradation factor, T be the sample time, S_1 be the fully successful state, and S_n be the fully failed state. Suppose $p_{ij}(t - T, t) \in P(t - T, t)$ represents the one-step transition probability from state S_i to state S_j at time $t - T$. For time t , the estimate of $p_{ij}(t, t + T) \in P(t, t + T)$ satisfies [42] [see (22) at the bottom of the page].

$$\hat{p}_{ij}(t, t + T) = \begin{cases} p_{ij}(t - T, t) \cdot \left(1 - \frac{\sum_{k=i+1}^n p_{ik}(t - T, t)}{i} \lambda(t) \right) & \text{if } j \leq i, \lambda(t) \in (0, 1). \\ p_{ij}(t - T, t) \cdot (1 + \lambda(t)) & \text{if } j > i \end{cases} \quad (22)$$

Proof: See the Appendix.

Remark 14: The value of $\lambda(t)$ reflects the speed of system degradation. If $p_{ij}(t - T, t)$ and $\lambda(t)$ are available, *Lemma 1* theoretically gives an approach to predict the one-step transition probability, which can further predict $\hat{R}(t + T | t)$ and $\hat{\Gamma}(t)$. However, according to *Remark 11*, (16) is used to calculate the multi-step transition probability rather than one-step transition probability considering the law of large numbers. Further, profust reliability reflects system performance over a time interval. In this case, even though $p_{ij}(t - T, t)$ is known, it is also improper to apply it to the prediction of $\hat{R}(t + T | t)$. On the other hand, the probability $\hat{P}(t, t + \Delta)$ cannot be estimated by $P(t - T, t)$ using a traditional Chapman-Kolmogorov equation because of the non-homogeneous property of the proposed Markov model [41]. Thus, an approach to the multi-step transition probability prediction is shown below.

Theorem 2: Let $\lambda(t)$ be a degradation factor, T be the sample time, S_1 be the fully successful state, and S_n be the fully failed state. Suppose $p_{ij}(t - \Delta, t) \in P(t - \Delta, t)$ represents the k -step transition probability from state S_i to state S_j over the time interval $[t - \Delta, t]$ ($\Delta = kT, k \in \mathbb{N}^+$). Then, for the time interval $[t, t + \Delta]$,

i) the estimate of transition probability $p_{ij}(t, t + \Delta) \in P(t, t + \Delta)$ satisfies [see (23) at the bottom of the next page]. ii) the estimate of state probability vector $\Phi(t + \Delta)$ satisfies

$$\hat{\Phi}(t + \Delta) = \hat{P}(t, t + \Delta) \cdot \Phi(t), \quad (24)$$

and iii) the estimate of profust reliability $R(t + \Delta | t)$ satisfies [see (25) at the bottom of the page].

Proof: See the Appendix.

Remark 15: In *Theorem 2*, the degradation factor $\lambda(t)$ is a time-varying variable different from that of *Lemma 1*, because, for a complex system, predictions made at an early stage have less information about the dynamics of fault evolution. A fixed degradation factor will lead to inaccurate RUL prediction. Thus, in the proposed approach, a numerical search method based on a least squares criterion is developed to determine $\lambda(t)$, as shown below.

For a specific system, assume that we can obtain n statistically independent profust reliability trajectories reflecting degradation processes of similar systems or the same technology family of products at a Δ sampling period written as $\{\Gamma_1, \Gamma_2, \dots, \Gamma_n\}$. At the current time t , a profust reliability trajectory $\Gamma_0(t)$ of the studied system ending at time t is easy to be obtained using *Theorem 1*. Comparing $\Gamma_0(t)$ with $\{\Gamma_1, \Gamma_2, \dots, \Gamma_n\}$, a set of normalized distance score

$D(t) = \{d_1(t), d_2(t), \dots, d_n(t); \sum_{i=1}^n d_i(t) = 1\}$ is obtained using the method in [43]. Because the degradation factor belongs to the range $(0, 1)$, with $\Gamma_i (i = 1, \dots, n)$, and a set of extended prediction of $\Gamma_0(t)$ over $\forall \lambda_i(t) \in (0, 1)$, the optimal $\lambda_i(t)$ can be found by numerical search based on a least squares criterion. Then, a weighted degradation factor of the proposed system at time t is defined as

$$\lambda(t) = \sum_{i=1}^n d_i(t) \lambda_i(t). \quad (26)$$

Remark 16: Using *Theorem 2*, a predicted profust reliability trajectory $\hat{\Gamma}(t)$, as shown in (21), is obtained at the current time t , and $\hat{r}(t)$ is further predicted using *Definition 5*. Because $\lambda(t)$ is a weighted value, the obtained $\hat{r}(t)$ is also a mean estimate. Here, the time interval Δ is identical to the estimation window, as shown in *Remark 12*. The length of Δ could also affect the RUL prediction performance. A smaller Δ will lead to a better result with high accuracy, but it also requires a longer run time. Additionally, it must be noted that (15) should be always satisfied when the transition probability matrix is updated by *Theorem 2*.

Corollary 1: Let $\lambda(t)$ be a degradation factor, T be the sample time, S_1 be the fully successful state, and S_n be the fully failed state. For the transition probability matrix $p_{ij}(t_0, t) \in P(t_0, t)$, suppose that

$$p_{ij}(t_0, t) = 0, \quad \text{if } j < i. \quad (27)$$

Then, for the transition probability $p_{ij}(t, t + \Delta) \in P(t, t + \Delta)$, we have (28) at the bottom of the next page.

$$\hat{p}_{ij}(t, t + \Delta) = \begin{cases} p_{ij}(t - \Delta, t) \cdot \left(1 - \frac{\sum_{k=i+1}^n p_{ik}(t - \Delta, t)}{i} \lambda(t) \right) & \text{if } j \leq i, \lambda(t) \in (0, 1) \\ p_{ij}(t - \Delta, t) \cdot (1 + \lambda(t)) & \text{if } j > i \end{cases} \quad (23)$$

$$\begin{aligned} & \hat{R}(t + \Delta | t) \\ &= 1 - \lim_{n \rightarrow \infty} \left\{ \left[\sum_{i=1}^n \sum_{j=1}^n \mu_{TSF}(m_{ij}) \cdot \hat{p}_{ij}(t, t + \Delta) \right] \cdot \left[\sum_{i=1}^n \mu_S(S_i) \cdot \phi_{S_i}(t) \right] - \sum_{i=1}^n \mu_F(S_i) \cdot \phi_{S_i}(t) \right\} \quad (25) \end{aligned}$$

Proof: See the Appendix.

Remark 17: Equation (27) is true for a degraded system without maintenance actions. This means that a transition will not occur from a worse state to a better state without maintenance actions. In this case, *Corollary 1* is more effective to predict $\hat{p}_{ij}(t, t + \Delta)$ than *Theorem 2* due to less calculation, which leads to a more efficient RUL prediction.

Theorem 2 and *Corollary 1* present the profust reliability prediction algorithm only for adjacent time intervals. *Corollary 2* gives a more general form below.

Corollary 2: Let $\lambda(t)$ be a degradation factor, T be the sample time, S_1 be the fully successful state, and S_n be the fully failed state. Suppose $p_{ij}(t - \Delta, t) \in P(t - \Delta, t)$ represents the k -step transition probability from state S_i to state S_j over the time interval $[t - \Delta, t]$ ($\Delta = kT, k \in \mathbb{N}^+$). Then, for $M \in \mathbb{N}^+$,

i) the estimate of transition probability $p_{ij}(t + (M - 1)\Delta, t + M\Delta) \in P(t + (M - 1)\Delta, t + M\Delta)$ satisfies [see (29) at the bottom of the page]. ii) the estimate of state probability vector $\Phi(t + M\Delta)$ satisfies [see (30) at the bottom of the page] and

iii) the estimate of profust reliability $R(t + M\Delta | t)$ satisfies [see (31) at the bottom of the page].

Proof: See the Appendix.

Remark 18: Both *Theorem 2* and *Corollary 1* are developed to achieve an iterative RUL prediction algorithm. Here, *Corollary 2* is developed for the prediction without multiple iterations, which is performed to search optimal $\lambda(t)$ with a higher efficiency than *Theorem 2*.

IV. A CASE STUDY: DEGRADATION OF LI-ION BATTERIES

In this section, the proposed PHM approach is implemented to study the degradation of Li-ion batteries. To make it self-contained, the health estimation part in [37] is also presented here. On this basis, the validation of the RUL prediction approach is proposed, and the experimental results are given and discussed. The data for Li-ion batteries are downloaded from the NASA Ames Prognostics Data Repository [38].

The battery data set recorded accelerated aging experiments of different batteries, which were run through repeated charge

$$\hat{p}_{ij}(t, t + \Delta) = \begin{cases} p_{ij}(t - \Delta, t) \cdot [1 + \lambda(t)] & \text{if } j > i \\ p_{ii}(t - \Delta, t) - \lambda(t) \cdot \sum_{k=i+1}^n p_{ik}(t - \Delta, t) & \text{if } j = i \\ 0 & \text{if } j < i \end{cases} \quad (28)$$

$$\begin{aligned} & \hat{p}_{ij}(t + (M - 1)\Delta, t + M\Delta) \\ &= \begin{cases} p_{ij}(t - \Delta, t) \cdot \prod_{l=1}^M \left\{ \frac{1 - [1 + \lambda(t)]^l \cdot \sum_{k=i+1}^n p_{ik}(t - \Delta, t)}{1 - [1 + \lambda(t)]^{l-1} \cdot \sum_{k=i+1}^n p_{ik}(t - \Delta, t)} \right\} & \text{if } j \leq i \\ p_{ij}(t - \Delta, t) \cdot [1 + \lambda(t)]^M & \text{if } j > i \end{cases} \end{aligned} \quad (29)$$

$$\begin{aligned} \hat{\Phi}(t + M\Delta) &= \hat{P}(t + (M - 1)\Delta, t + M\Delta) \cdot \hat{\Phi}(t + (M - 1)\Delta) \\ &= P(t - \Delta, t) \cdot \prod_{l=1}^M \hat{P}(t + (l - 1)\Delta, t + l\Delta) \cdot \Phi(t) \end{aligned} \quad (30)$$

$$\begin{aligned} & \hat{R}(t + M\Delta | t) \\ &= 1 - \lim_{n \rightarrow \infty} \left\{ \frac{\left[\sum_{i=1}^n \sum_{j=1}^n \mu_{TS^r}(m_{ij}) \cdot \hat{p}_{ij}(t + (M - 1)\Delta, t + M\Delta) \right]}{\left[\sum_{i=1}^n \mu_S(S_i) \cdot \hat{\phi}_{S_i}(t + (M - 1)\Delta) \right] - \sum_{i=1}^n \mu_F(S_i) \cdot \hat{\phi}_{S_i}(t + (M - 1)\Delta)} \right\} \end{aligned} \quad (31)$$

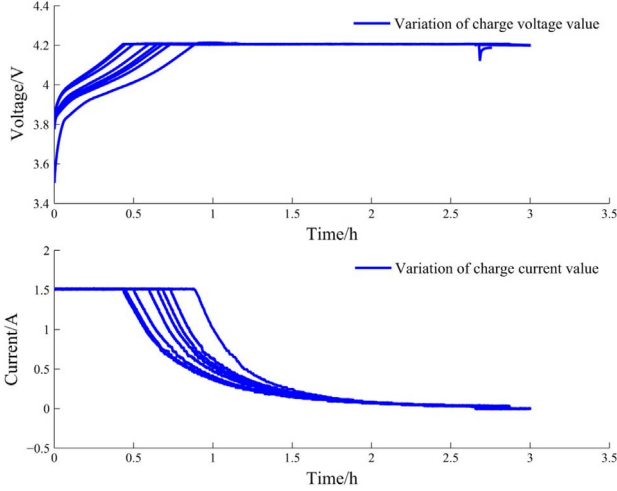


Fig. 5. Variations of charge voltage and current values.

and discharge cycles at different ambient temperatures. The experiments were stopped until the battery capacity dropped to 70% of the rated value. Here, we mainly concentrate on the charge cycles. Charging was carried out in a constant current (CC) mode at 1.5 A until the battery voltage reached 4.2 V, and then continued in a constant voltage (CV) mode until the charge current dropped to 20 mA. Through studying the battery performance during each charge cycle, the battery health status after completely charging is estimated, and the estimate of remaining charge cycles (RCC) is predicted using the proposed approach. By taking battery #5 as an example, the data contain 167 whole charge cycles. For ease of visualization, variations of charge voltage and current of 8 charge cycles are shown in Fig. 5.

Here, let $u(t)$, and $i(t)$ represent the corresponding voltage variable, and current variable, respectively. To consider both $u(t)$ and $i(t)$, the battery charge capacity $Q(t)$ is considered as an assessable index for battery health estimation, which is defined as

$$Q(t) = \int_0^t u(\tau) \cdot i(\tau) d\tau, \quad (32)$$

where the unit of $Q(t)$ is $V\text{Ahr}$. Then, the real-time charge capacity of all 167 charge cycles are calculated using (32). Similarly, the real-time charge capacity of the preceding 8 charge cycles are shown in Fig. 6.

In practice, the first charge cycle after fully discharging is able to charge the battery to the maximum capacity, which is corresponding to the highest curve in Fig. 6. In this case, we consider it as the fully successful state of the battery charge process, which is also viewed as a standard charge cycle. Furthermore, it is considered that the battery starts to degrade after the first charge cycle. Let $e(t)$ represent the real-time error that the charge capacity of each charge cycle deviates from the standard curve with time. Then, for each charge cycle C_k , we have

$$e_k(t) = Q_1(t) - Q_k(t), \quad k = 1, 2, 3, \dots, 167. \quad (33)$$

As shown in Fig. 7, $e(t)$ is a continuous signal which is viewed as a continuous system state. According to Remark 10,

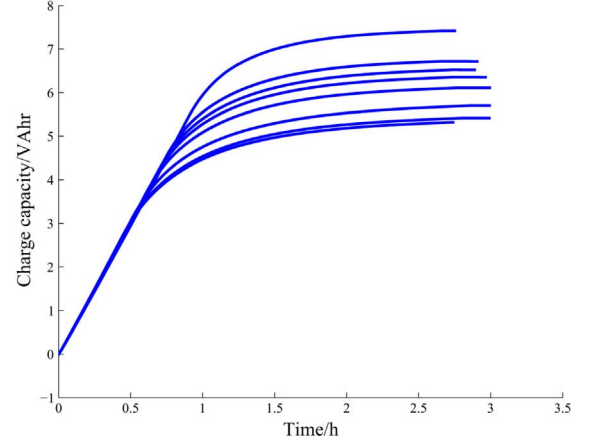


Fig. 6. Charge capacity variation.

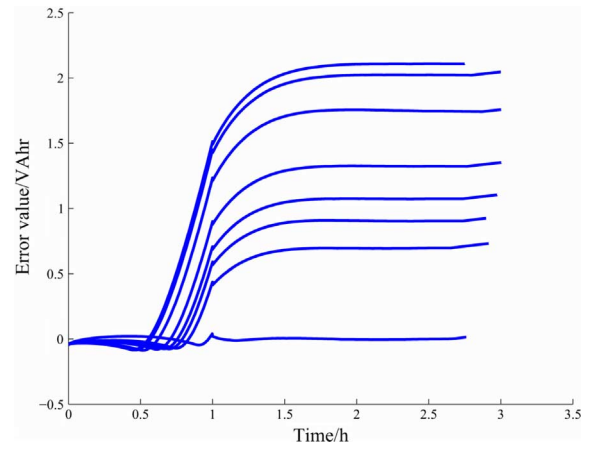


Fig. 7. Error variation.

a trapezoidal membership function is selected to be the fuzzy success membership function $\mu_S(e(t))$, because $e(t)$ is always required to be 0 if the battery is in a fully successful state. Then, through analyzing historical data of similar batteries, thresholds of the proposed trapezoidal membership function are given,

$$\mu_S(e(t)) = \begin{cases} \frac{e(t)+2}{1.5} & e(t) \in (-2, -0.5] \\ 1 & e(t) \in (-0.5, 0.5] \\ \frac{e(t)-2}{-1.5} & e(t) \in (0.5, 2] \\ 0 & e(t) \in (-\infty, -2] \cup (2, +\infty) \end{cases} \quad (34)$$

and

$$\mu_F(e(t)) = 1 - \mu_S(e(t)). \quad (35)$$

Then, following the implementation steps in Section III, we can estimate the profust reliability at the time when a complete charge is finished, and predict the number of remaining charge cycles.

A. Discretization

For simplicity, $|e(t)|$ is employed to represent a continuous system state instead of $e(t)$, because $\mu_S(e(t))$ is an even function. Let $U = \{|e(t)| \mid |e(t)| \geq 0\}$. For $U_1 = \{|e(t)| \mid 0 \leq |e(t)| \leq 2\}$, $U_1 \subset U$, let

$$S_i = \{|e(t)| \mid a_{i-1} \leq |e(t)| \leq a_i\},$$

where

$$\delta = \frac{2}{n}, n = 50, a_i = 0 + i \cdot \delta, i = 1, 2, \dots, 50.$$

Considering $\exists |e(t)| \notin U_1$ in the domain U , let

$$S_{51} = \{|e(t)| \mid |e(t)| \notin U_1, |e(t)| \in U\}.$$

In this case, S_1 is the fully successful state, and S_{51} is the fully failed state. Then, according to *Theorem 1*, the profust reliability of the k th charge cycle C_k is computed as (36) at the bottom of the page, where $p_{ij,k}(t_{s,k}, t_{e,k})$ represents the transition probability from state S_i to state S_j over the charge cycle C_k ; $\phi_{S_i,k-1}(t_{e,k-1})$ represents the state probability of system state S_i at the time when the charge cycle C_{k-1} is completely finished. The times $t_{s,k}$ and $t_{e,k}$ represent the start and end times of the charge cycle C_k , respectively. Here, for sake of simplicity, we take the charge cycles as a continuous process. Then, we have $t_{s,k} = t_{e,k-1}$.

B. Transition Probability, and State Probability Calculations

After state discretization, the transition probability $p_{ij}(\cdot) \in P$, and state probability $\phi_{S_i}(\cdot) \in \Phi$ are easy to obtain through (16), and (18), respectively. For the charge cycle C_k , we have

$$p_{ij,k}(t_{s,k}, t_{e,k}) = \frac{n_{ij,k}(t_{s,k}, t_{e,k})}{\sum_{j=1}^{51} n_{ij,k}(t_{s,k}, t_{e,k})}, \quad (37)$$

and

$$\Phi_k(t_{e,k}) = P_k(t_{s,k}, t_{e,k}) \cdot \Phi_{k-1}(t_{e,k-1}), \quad (38)$$

where $n_{ij,k}(t_{s,k}, t_{e,k})$ represents the number of transitions from state S_i to state S_j over the charge cycle C_k . Here, the state probability vector $\Phi_{k-1}(t_{e,k-1})$ is obtained from the charge cycle C_{k-1} .

C. Health Estimation

Let a charge cycle C be the estimation window, which is moving each charge cycle as shown in Fig. 4(b). Then, following the two steps above, a profust reliability trajectory is obtained as

$$\Gamma = \{R(1), R(2), \dots, R(k), \dots, R(167)\}$$

According to *Remark 8*, let $R = 0.4$ be the failure threshold in this case. The result is shown in Fig. 8.

Remark 19: The curve in Fig. 8 should be monotonically non-increasing with charge cycle, because the health status of the

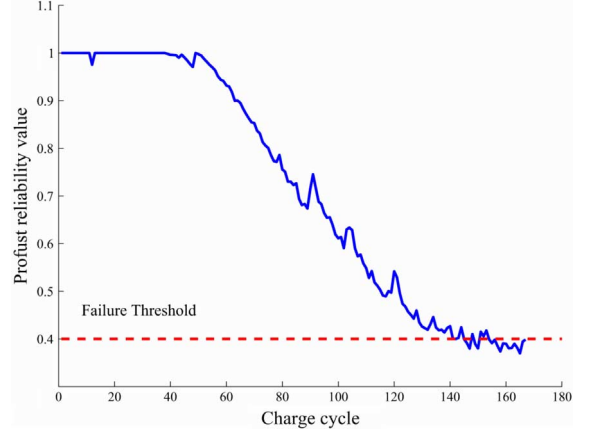


Fig. 8. Profust reliability value variation of all charge cycles.

battery should decrease over time. However, the charge capacity of each charge cycle is not monotonically decreasing in accelerated aging experiments because the experimental process contains various uncertainties. For example, incomplete discharge may occur in discharge cycles, and an unstable chemical reaction inside the battery will also lead to fluctuations of charge capacity. Thus, these system uncertainties will eventually lead to fluctuations of $R(t)$ in a small range.

D. RUL Prediction

In this case study, the number of RCC is discussed as RUL. In the battery data set [38], batteries #5, #6, #7, #18 were run in the same environment, and degraded in similar patterns. Here, the profust reliability trajectories $\{\Gamma_6, \Gamma_7, \Gamma_{18}\}$ of batteries #6, #7, #18 are used to find the optimal $\lambda(k)$ as reference trajectories, and the profust reliability data of battery #5 is used to test the RCC prediction. Fig. 9 shows the 3 reference trajectories, and the testing trajectory.

For battery #5 at a specific charge cycle C_k , let $\Gamma_5(k) = \{R(k-19), \dots, R(k)\}$ be a 20-long segment of profust reliability trajectory calculated by *Theorem 1*. Comparing $\{\Gamma_6, \Gamma_7, \Gamma_{18}\}$ with $\Gamma_5(k)$ by [43], a set of normalized distance scores $D(k)$ is obtained as

$$D(k) = \{d_6(k), d_7(k), d_{18}(k); d_6(k) + d_7(k) + d_{18}(k) = 1\}.$$

Then, the optimal $\lambda_i(k)$ ($i = 6, 7, 18$) can be derived from a numerical search over $(0, 1)$, and $\lambda_5(k)$ of the battery #5 at time t is calculated by (26) as

$$\lambda_5(k) = \sum_{i \in \{6, 7, 18\}} d_i(k) \cdot \lambda_i(k).$$

$$R(k) = 1 - \left[\sum_{i=1}^{51} \sum_{j=1}^{51} \mu_{T_{SF}}(m_{ij}) \cdot p_{ij,k}(t_{s,k}, t_{e,k}) \right] \cdot \left[\sum_{i=1}^{51} \mu_S(S_i) \cdot \phi_{S_i,k-1}(t_{e,k-1}) \right] - \sum_{i=1}^{51} \mu_F(S_i) \cdot \phi_{S_i,k-1}(t_{e,k-1}) \quad (36)$$

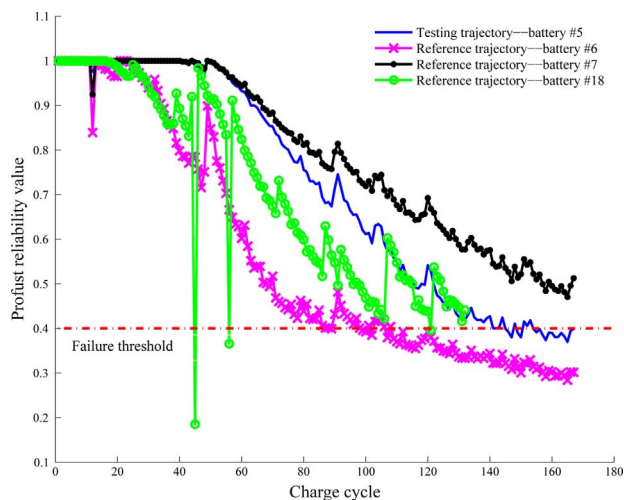


Fig. 9. Profust reliability trajectories used for RUL prediction.

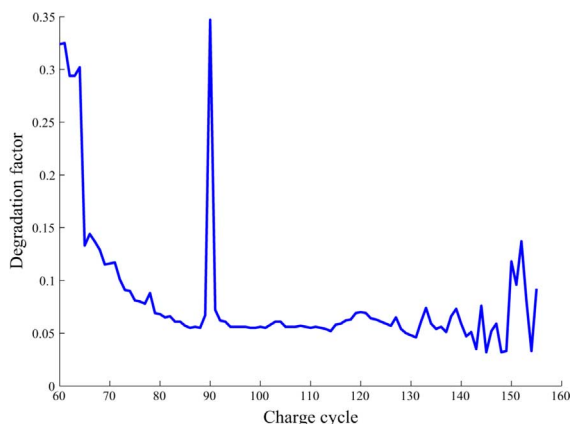


Fig. 10. Degradation factor variation.

After getting $\lambda_5(k)$, a predicted profust reliability trajectory, and a mean value of \hat{r}_c can be obtained using *Theorem 2*. The aforementioned $R = 0.4$ was chosen as the failure threshold in this case. Actually, from Fig. 8, the profust reliability curve fluctuates around 0.4 over charge cycles [142, 167]. Here, assume that, after the charge cycle C_{155} is complete, $r_c = 0$. Further, assume the prediction starts at the time when the charge cycle C_{60} is complete in this case. Then, multiple predictions are generated starting from the charge cycle C_{60} to C_{155} of battery #5. Then, for the charge cycle C_k ($k = 60, \dots, 155$), the experimental results of $\lambda_5(k)$ are shown in Fig. 10, and the corresponding mean value of \hat{r}_c is shown in Fig. 11.

To quantify the RCC prediction performance, several prognostics metrics are implemented in this case, including accuracy, precision, prognostic horizon (PH), α - λ performance, and relative accuracy (RA), as shown in Table I. Interested readers can get more details from [44]. Fig. 12 shows the absolute error of each prediction for a more intuitive evaluation.

From Figs. 11 and 12, it can be observed that the prediction at an early stage is unsatisfied due to less information about the degradation pattern as compared with predicting at a later stage. However, the mean value of \hat{r}_c converges to the true r_c (with a 20% confidence interval) after the 93th charge cycle. Then, after the 140th charge cycle, the mean \hat{r}_c fluctuates in a small range, which is similar to the health estimation result of the battery

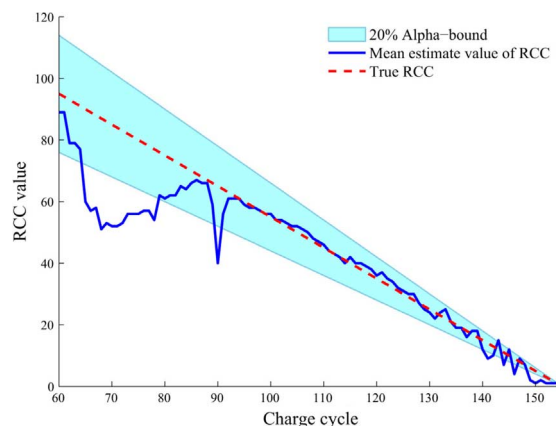


Fig. 11. RCC prediction of the battery #5.

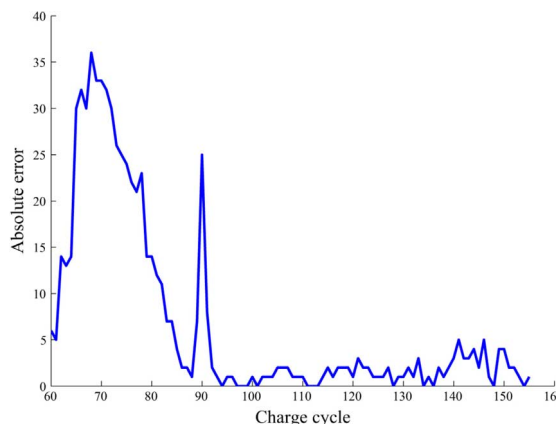


Fig. 12. Absolute error of all predictions.

#5 in Fig. 8. The experimental results show that the proposed approach can be effectively used to estimate battery health status and predict remaining charge cycles.

V. CONCLUSION

This paper presents a data-driven PHM approach based on profust reliability theory, where profust reliability is used to evaluate the real-time system performance as a unified health indicator for different kinds of systems. On the basis of the health estimation results, RUL is predicted using a degraded Markov model. To show effectiveness of the proposed approach, the degradation process of Li-ion batteries is studied. The experimental results show that the battery health status can be effectively estimated, and the number of remaining charge cycles can be estimated in an accepted error range. In our future works, system models will be taken into consideration for a better health estimation and RUL prediction.

APPENDIX

A. Proof of Theorem 1

For a continuous domain $U = \{x \mid a \leq x \leq b\}$, let

$$S_i = \{x \mid a_{i-1} \leq x \leq a_i\}$$

where

$$\delta = \frac{b-a}{n}, a_i = a + i \cdot \delta, i = 1, 2, \dots, n.$$

TABLE I
 PERFORMANCE EVALUATION FOR THE RCC PREDICTION

Accuracy	Precision	PH	α - λ performance($\alpha = 0.2, \lambda = 0.5$)	RA($\lambda = 0.25$)	RA($\lambda = 0.5$)
6.854	9.957	76	TRUE	0.8611	0.9365

Then

$$U = \lim_{n \rightarrow \infty} \bigcup_{i=1}^n \{S_i\}$$

correspondingly, (1) and (2) become

$$S = \lim_{n \rightarrow \infty} \bigcup_{i=1}^n \{S_i, \mu_S(S_i)\} \doteq \lim_{n \rightarrow \infty} \bigcup_{i=1}^n \{S_i, \mu_S(a_i)\}$$

$$F = \lim_{n \rightarrow \infty} \bigcup_{i=1}^n \{S_i, \mu_F(S_i)\} \doteq \lim_{n \rightarrow \infty} \bigcup_{i=1}^n \{S_i, \mu_F(a_i)\},$$

where

$$\mu_S(S_i) = \frac{1}{\delta} \int_{a_{i-1}}^{a_i} \mu_S(x) dx$$

$$\mu_F(S_i) = \frac{1}{\delta} \int_{a_{i-1}}^{a_i} \mu_F(x) dx.$$

Equation (5) becomes

$$T_{SF} = \{m_{ij}, \mu_{T_{SF}}(m_{ij}), i, j = 1, 2, \dots, n\},$$

where

$$\mu_{T_{SF}}(m_{ij}) = \frac{1}{\delta} \int_{a_{i-1}}^{a_i} \left[\frac{1}{\delta} \int_{a_{i-1}}^{a_i} \mu_{T_{SF}}(m_{xy}) dy \right] dx,$$

$$\mu_{T_{SF}}(m_{ij}) = \begin{cases} \beta_{F|S}(S_j) - \beta_{F|S}(S_i) & \text{if } \beta_{F|S}(y) > \beta_{F|S}(S_i) \\ 0 & \text{otherwise} \end{cases}$$

$$\beta_{F|S}(S_i) = \frac{\mu_F(S_i)}{\mu_S(S_i) + \mu_F(S_i)}.$$

Then, (10) becomes the equation at the bottom of the page.

B. Membership Function Calculation of a Complex System

Generally, a complex system contains various components and parameters. In this case, the weight of parameters and the topological structure of the system should be taken into consideration when operating PHM. For a single component, the membership function is the weighted sum of each parameter's membership. Then, supposing the operational state of component A to be determined by parameters $\{a_1, a_2, \dots, a_n\}$, the membership function of component A is obtained as

$$\mu_A = \sum_{i=1}^n w_i \cdot \mu(a_i),$$

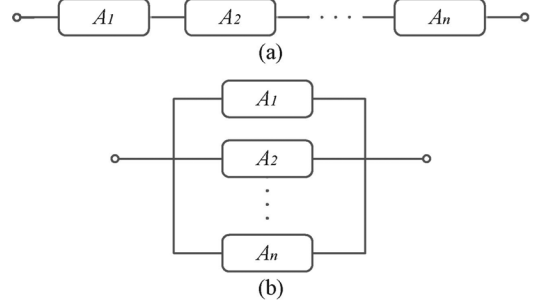


Fig. 13. System structure: (a) series system, (b) parallel system.

where $\mu(a_i)$ represents the membership function of parameter a_i , w_i represents the weight of parameter a_i in component A , fulfilling the condition

$$\sum_{i=1}^n w_i = 1, w_i \in [0, 1].$$

Let $\mu_S^{(i)}$, and $\mu_F^{(i)}$ be the fuzzy success, and failure membership functions of component A_i in a complex system, respectively. Consider a series system in Fig. 13(a), we have

$$\mu_S = \prod_{i=1}^n \mu_S^{(i)}$$

$$\mu_F = 1 - \prod_{i=1}^n (1 - \mu_F^{(i)}).$$

Considering a parallel system in Fig. 13(b), we have

$$\mu_S = 1 - \prod_{i=1}^n (1 - \mu_S^{(i)})$$

$$\mu_F = \prod_{i=1}^n \mu_F^{(i)}.$$

C. Proof of Lemma 1

For the transition probability $p_{ij}(\cdot) \in P(\cdot)$, we have

$$p_{ij}(t, t+T) - p_{ij}(t-T, t) > 0 \text{ if } j > i,$$

and

$$p_{ij}(t, t+T) - p_{ij}(t-T, t) \leq 0 \text{ if } j \leq i.$$

$$R(t) = 1 - \lim_{n \rightarrow \infty} \left\{ \left[\sum_{i=1}^n \sum_{j=1}^n \mu_{T_{SF}}(m_{ij}) \cdot p_{ij}(t) \right] \cdot \left[\sum_{i=1}^n \mu_S(S_i) \cdot \phi_{S_i}(t_0) \right] - \sum_{i=1}^n \mu_F(S_i) \cdot \phi_{S_i}(t_0) \right\}$$

From (15), we have

$$\sum_{k=1}^n p_{ik}(\cdot) = 1.$$

Thus, we have (39) at the bottom of the page. Here, a degradation factor $\lambda(t) \in (0, 1)$ is defined. $\forall t$,

$$\lambda(t) = \frac{\sum_{k=i+1}^n p_{ik}(t, t+T) - \sum_{k=i+1}^n p_{ik}(t-T, t)}{\sum_{k=i+1}^n p_{ik}(t-T, t)}, \quad (40)$$

where $\lambda(t)$ represents the increase rate in $\sum_{k=i+1}^n p_{ik}(\cdot)$ for a system becoming degraded.

Then,

$$\sum_{k=i+1}^n p_{ik}(t, t+T) - \sum_{k=i+1}^n p_{ik}(t-T, t) = \lambda(t) \cdot \sum_{k=i+1}^n p_{ik}(t-T, t).$$

For each element $p_{ij}(\cdot)$, if $j > i$, we have (41) shown at the bottom of the page, and if $j \leq i$, combining (39) and (40), we have (42) shown at the bottom of the page.

Then, we have (see the last equation at the bottom of the page).

D. Proof of Theorem 2

Referring to Lemma 1, for the transition probability $p_{ij}(t, t+\Delta) \in P(t, t+\Delta)$, we have we have (43) shown at the bottom of the page, where $\lambda(t) \in (0, 1)$. For the state probability vector $\Phi(t+\Delta)$,

$$\widehat{\Phi}(t+\Delta) = \widehat{P}(t, t+\Delta) \cdot \Phi(t).$$

$$\sum_{k=i+1}^n p_{ik}(t, t+T) - \sum_{k=i+1}^n p_{ik}(t-T, t) = \sum_{k=1}^i p_{ik}(t-T, t) - \sum_{k=1}^i p_{ik}(t, t+T) \quad (39)$$

$$\begin{aligned} p_{ij}(t, t+T) - p_{ij}(t-T, t) &= \frac{p_{ij}(t-T, t)}{\sum_{k=i+1}^n p_{ik}(t-T, t)} \left(\sum_{k=i+1}^n p_{ik}(t, t+T) - \sum_{k=i+1}^n p_{ik}(t-T, t) \right) \\ &= p_{ij}(t-T, t) \cdot \lambda(t); \end{aligned} \quad (41)$$

$$\begin{aligned} p_{ij}(t-T, t) - p_{ij}(t, t+T) &= \frac{p_{ij}(t-T, t)}{\sum_{k=1}^i p_{ik}(t-T, t)} \left(\sum_{k=1}^i p_{ik}(t-T, t) - \sum_{k=1}^i p_{ik}(t, t+T) \right) \\ &= \frac{\sum_{k=i+1}^n p_{ik}(t-T, t)}{\sum_{k=1}^i p_{ik}(t-T, t)} \lambda(t) \end{aligned} \quad (42)$$

$$\widehat{p}_{ij}(t, t+T) = \begin{cases} p_{ij}(t-T, t) \cdot \left(1 - \frac{\sum_{k=i+1}^n p_{ik}(t-T, t)}{\sum_{k=1}^i p_{ik}(t-T, t)} \lambda(t) \right) & \text{if } j \leq i, \lambda(t) \in (0, 1). \\ p_{ij}(t-T, t) \cdot (1 + \lambda(t)) & \text{if } j > i \end{cases}$$

Correspondingly, substituting (43) into (14), we have the second equation at the bottom of the page.

E. Proof of Corollary 1

According to (27), we have

$$\begin{cases} p_{ij} = p_{ii} = \sum_{k=1}^i p_{ik}(t - \Delta, t) & \text{if } j = i \\ p_{ij} = 0 & \text{if } j < i \end{cases}$$

For $j \leq i$, (40) becomes

$$\lambda(t) = \frac{p_{ii}(t - \Delta, t) - p_{ii}(t, t + \Delta)}{\sum_{k=i+1}^n p_{ik}(t - \Delta, t)} \text{ for } \forall t.$$

Then, (23) becomes the third equation at the bottom of the page.

F. Proof of Corollary 2

For simplicity, let $p_{ij}(M - 1, M)$ represent $p_{ij}(t + (M - 1)\Delta, t + M\Delta)$, and $p_{ij}(0)$ represent $p_{ij}(t - \Delta, t)$.

From *Theorem 2*, for $j > i$,

$$\begin{aligned} p_{ij}(M - 1, M) &= p_{ij}(M - 2, M - 1) \cdot [1 + \lambda(t)] \\ &= \cdots = p_{ij}(0) \cdot [1 + \lambda(t)]^M; \end{aligned}$$

for $j \leq i$, see (44) at the bottom of the page, where, see (45) at the bottom of the page.

$$\hat{p}_{ij}(t, t + \Delta) = \begin{cases} p_{ij}(t - \Delta, t) \cdot \left(1 - \frac{\sum_{k=i+1}^n p_{ik}(t - \Delta, t)}{\sum_{k=1}^i p_{ik}(t - \Delta, t)} \lambda(t) \right) & \text{if } j \leq i \\ p_{ij}(t - \Delta, t) \cdot (1 + \lambda(t)) & \text{if } j > i \end{cases} \quad (43)$$

$$\begin{aligned} &\hat{R}(t + \Delta | t) \\ &= 1 - \lim_{n \rightarrow \infty} \left\{ \left[\sum_{i=1}^n \sum_{j=1}^n \mu_{TSF}(m_{ij}) \cdot \hat{p}_{ij}(t, t + \Delta) \right] \cdot \left[\sum_{i=1}^n \mu_S(S_i) \cdot \phi_{S_i}(t) \right] - \sum_{i=1}^n \mu_F(S_i) \cdot \phi_{S_i}(t) \right\} \end{aligned}$$

$$\hat{p}_{ij}(t, t + \Delta) = \begin{cases} p_{ij}(t - \Delta, t) \cdot (1 + \lambda(t)) & \text{if } j > i \\ p_{ii}(t - \Delta, t) - \lambda(t) \cdot \sum_{k=i+1}^n p_{ik}(t - \Delta, t) & \text{if } j = i \\ 0 & \text{if } j < i \end{cases}$$

$$p_{ij}(M - 1, M) = p_{ij}(M - 2, M - 1) \cdot \left(1 - \frac{\sum_{k=i+1}^n p_{ik}(M - 2, M - 1)}{\sum_{k=1}^i p_{ik}(M - 2, M - 1)} \lambda(t) \right) \quad (44)$$

$$\frac{\sum_{k=i+1}^n p_{ik}(M - 2, M - 1)}{\sum_{k=1}^i p_{ik}(M - 2, M - 1)} = \frac{\sum_{k=i+1}^n p_{ik}(M - 2, M - 1)}{1 - \sum_{k=i+1}^n p_{ik}(M - 2, M - 1)} = \frac{[1 + \lambda(t)]^{M-1} \cdot \sum_{k=i+1}^n p_{ik}(0)}{1 - [1 + \lambda(t)]^{M-1} \cdot \sum_{k=i+1}^n p_{ik}(0)} \quad (45)$$

$$\begin{aligned}
p_{ij}(M-1, M) &= p_{ij}(M-2, M-1) \cdot \left(1 - \frac{[1 + \lambda(t)]^{M-1} \cdot \sum_{k=i+1}^n p_{ik}(0)}{1 - [1 + \lambda(t)]^{M-1} \cdot \sum_{k=i+1}^n p_{ik}(0)} \lambda(t) \right) \\
&= p_{ij}(M-2, M-1) \cdot \frac{1 - [1 + \lambda(t)]^M \cdot \sum_{k=i+1}^n p_{ik}(0)}{1 - [1 + \lambda(t)]^{M-1} \cdot \sum_{k=i+1}^n p_{ik}(0)} \\
&= \dots = p_{ij}(0) \cdot \prod_{l=1}^M \left\{ \frac{1 - [1 + \lambda(t)]^l \cdot \sum_{k=i+1}^n p_{ik}(0)}{1 - [1 + \lambda(t)]^{l-1} \cdot \sum_{k=i+1}^n p_{ik}(0)} \right\}
\end{aligned}$$

$$\begin{aligned}
&\widehat{p}_{ij}(t + (M-1)\Delta, t + M\Delta) \\
&= \begin{cases} p_{ij}(t - \Delta, t) \cdot \prod_{l=1}^M \left\{ \frac{1 - [1 + \lambda(t)]^l \cdot \sum_{k=i+1}^n p_{ik}(t - \Delta, t)}{1 - [1 + \lambda(t)]^{l-1} \cdot \sum_{k=i+1}^n p_{ik}(t - \Delta, t)} \right\} & \text{if } j \leq i, \\ p_{ij}(t - \Delta, t) \cdot [1 + \lambda(t)]^M & \text{if } j > i \end{cases}, \quad (46)
\end{aligned}$$

$$\begin{aligned}
&\widehat{R}(t + M\Delta | t) \\
&= 1 - \lim_{n \rightarrow \infty} \left\{ \left[\sum_{i=1}^n \sum_{j=1}^n \mu_{T_{SF}}(m_{ij}) \cdot \widehat{p}_{ij}(t + (M-1)\Delta, t + M\Delta) \right] \right. \\
&\quad \left. \cdot \left[\sum_{i=1}^n \mu_S(S_i) \cdot \widehat{\phi}_{S_i}(t + (M-1)\Delta) \right] - \sum_{i=1}^n \mu_F(S_i) \cdot \widehat{\phi}_{S_i}(t + (M-1)\Delta) \right\}
\end{aligned}$$

$$\begin{aligned}
\widehat{\Phi}(t + M\Delta) &= \widehat{P}(t + (M-1)\Delta, t + M\Delta) \cdot \widehat{\Phi}(t + (M-1)\Delta) \\
&= \dots = P(t - \Delta, t) \cdot \prod_{l=1}^M \widehat{P}(t + (l-1)\Delta, t + l\Delta) \cdot \Phi(t)
\end{aligned}$$

Equations (44) and (45) are simultaneously solved, so (see the second equation on the next page).

Thus [see (46) on the next page], where $\lambda(t) \in (0, 1)$, $M \in \mathbb{N}^+$, $M \neq 1$. For the state probability vector $\Phi(t + M\Delta)$, see the third equation on the next page.

Correspondingly, the estimate of profust reliability $R(t + M\Delta)$ satisfies that, see the last equation on the page.

ACKNOWLEDGMENT

The authors appreciate the anonymous reviewers and Guest Editors for their helpful comments & suggestions that greatly improve this paper.

REFERENCES

- [1] P. W. Kalgren, C. S. Byington, M. J. Roemer, and M. J. Watson, "Defining PHM, a lexical evolution of maintenance and logistics," in *Proc. IEEE Autotestcon Conf.*, 2006, pp. 353–358.

- [2] J. W. Sheppard and M. A. Kaufman, "IEEE standards for prognostics and health management," *IEEE Aerospace Electron. Syst. Mag.*, vol. 24, no. 9, pp. 34–41, 2009.
- [3] J. Dai, D. Das, and M. Pecht, "Prognostics-based risk mitigation for telecom equipment under free air cooling conditions," *App. Energy*, vol. 99, pp. 423–429, 2012.
- [4] E. Dolev, "Introduction to the special section on prognostics and health management," *IEEE Trans. Rel.*, vol. 58, no. 2, pp. 262–263, Jun. 2009.
- [5] M. Pecht and J. Gu, "Physics-of-failure-based prognostics for electric products," *Trans. Inst. Measur. Contr.*, vol. 31, no. 3–4, pp. 309–322, 2009.
- [6] A. Ramakrishnan and M. Pecht, "A life consumption monitoring methodology for electronic systems," *IEEE Trans. Compon. Packag. Technol.*, vol. 26, no. 3, pp. 625–634, 2003.
- [7] C. Y. Yin, M. Musallam, C. Bailey, and C. M. Johnson, "A physics-of-failure based prognostic method for power modules," in *Proc. 10th Electron. Packaging Technol. Conf.*, 2008, pp. 1190–1195.
- [8] K. Kulkarni, G. Biswas, and X. Koutsoukos, "Physics of failure models for capacitor degradation in DC-DC converters," in *Maintenance Rel. Conf.*, 2010, pp. 1–13.
- [9] J. Shao, C. Zeng, and Y. Wang, "Research progress on physics-of-failure based fatigue stress-damage model of solder joints in electronic packaging," in *Proc. Prognostics Health Management Conf.*, 2010.
- [10] H. Oh, M. H. Azarian, M. Pecht, and C. H. White, "Physics-of-failure approach for fan PHM in electronics applications," in *Proc. Int. Conf. Prognostics Health Manag.*, 2010.
- [11] M. Pecht, *Prognostics and Health Management of Electronics*. New York, NY, USA: Wiley-Interscience, 2008.
- [12] N. Blonder, H. Qiu, N. Eklund, and E. Hindle, "Physics-based remaining useful life prediction for aircraft engine bearing prognosis," in *Proc. Annu. Conf. Prognostics Health Management Soc.*, 2009.
- [13] C. S. Byington, M. Watson, and D. Edwards, "A model-based approach to prognostics and health management for flight control actuators," in *Proc. IEEE Aerospace Conf.*, 2004, vol. 6, pp. 3551–3562.
- [14] M. Schwabacher and K. Goebel, "A survey of artificial intelligence for prognostics," in *Proc. AAI Fall Symp.*, 2007.
- [15] J. Rafiee, F. Arvani, A. Harifi, and M. H. Sadeghi, "Intelligent condition monitoring of a gearbox using artificial neural network," *Mechan. Syst. Signal Process.*, vol. 21, no. 4, pp. 1746–1754, 2007.
- [16] N. Z. Gebrael and M. A. Lawley, "A neural network degradation model for computing and updating residual life distributions," *IEEE Trans. Autom. Sci. Eng.*, vol. 5, no. 1, pp. 154–163, 2008.
- [17] R. Huang, L. Xi, X. Li, and C. R. Liu, "Residual life predictions for ball bearings based on self-organizing map and back propagation neural network methods," *Mechan. Syst. Signal Process.*, vol. 21, no. 1, pp. 193–207, 2007.
- [18] H. R. Berenji and Y. Wang, "Wavelet neural networks for fault diagnosis and prognosis," in *Proc. IEEE Int. Conf. Fuzzy Syst.*, 2006, pp. 1334–1339.
- [19] C. S. Byington, M. Watson, and D. Edwards, "Data-driven neural network methodology to remaining life predictions for aircraft actuator components," in *Proc. IEEE Aerospace Conf.*, 2004, vol. 6, pp. 3581–3589.
- [20] S. Ogaji and R. Singh, "Artificial neural networks in fault diagnosis: A gas turbine scenario," *Comput. Intell. Fault Diagnosis*, pp. 179–207, 2006.
- [21] P. Wang and B. D. Youn, "A generic Bayesian framework for real-time prognostics and health management (PHM)," in *Proc. 50th AIAA/ASME/ASCE/AHS/ASC Structures, Structural Dynamics, Materials Conf. (AIAA 2009-2109)*, pp. 1–16.
- [22] D. A. Tobon-Mejia, K. Medjaher, N. Zerhouni, and G. Tripot, "A data-driven failure prognostics method based on mixture of Gaussians hidden Markov models," *IEEE Trans. Rel.*, vol. 61, no. 2, pp. 491–503, Jun. 2012.
- [23] M. Dong and D. He, "Hidden semi-Markov model-based methodology for multi-sensor equipment health diagnosis and prognosis," *Eur. J. Operational Res.: Stochastics Statist.*, vol. 178, no. 3, pp. 858–878, 2007.
- [24] C. S. Byington, P. W. Kalgen, R. Johns, and R. J. Beers, "Embedded diagnostic/prognostic reasoning and information continuity for improved avionics maintenance," in *Proc. IEEE Syst. Readiness Technol. Conf.*, 2003, pp. 320–329.
- [25] R. Jaai and M. Pecht, "Fusion prognostics," in *Proc. Sixth DSTO Int. Conf. Health & Usage Monitoring*, Melbourne, Australia, 2009.
- [26] J. Dai, D. Das, and M. Pecht, "Prognostics-based health management for free air cooling of data centers," in *Proc. IEEE Prognostics Health Management Conf.*, Macau, China, 2010.
- [27] J. R. Celaya, C. Kulkarni, G. Biswas, S. Saha, and K. Goebel, "A model-based prognostics methodology for electrolytic capacitors based on electrical overstress accelerated aging," in *Proc. Annu. Conf. Prognostics Health Management Soc.*, 2011.
- [28] P. W. Kalgren, M. Baybutt, A. Ginart, and C. Minnella, "Application of prognostic health management in digital systems," in *Proc. IEEE Aerospace Conf.*, 2007.
- [29] L. Peel, "Data driven prognostics using a Kalman filter ensemble of neural network models," in *Proc. Int. Conf. Prognostics Health Management*, 2008.
- [30] K.-Y. Cai, *Introduction to Fuzzy Reliability*. New York, NY, USA: Kluwer Academic Publishers, 1996.
- [31] K.-Y. Cai, C. Y. Wen, and M. L. Zhang, "Fuzzy reliability modeling of gracefully degradable computing systems," *Rel. Eng. Syst. Safety*, vol. 33, no. 1, pp. 141–157, 1991.
- [32] H. Lu, W. J. Kolarik, and S. S. Lu, "Real-time performance reliability prediction," *IEEE Trans. Rel.*, vol. 50, no. 4, pp. 353–357, Dec. 2001.
- [33] Z. Li and K. C. Kapur, "Continuous-state reliability measures based on fuzzy sets," *IEE Trans.: Quality Rel. Eng.*, vol. 44, no. 11, pp. 1033–1044, 2012.
- [34] Y. Liu and H. Z. Huang, "Reliability assessment for fuzzy multi-state systems," *Int. J. Syst. Sci.*, vol. 41, no. 4, pp. 365–379, 2010.
- [35] Y. Ding, M. J. Zuo, A. Lisnianski, and W. Li, "A framework for reliability approximation of multi-state weighted k -out-of- n systems," *IEEE Trans. Rel.*, vol. 59, no. 2, pp. 297–308, Jun. 2010.
- [36] Y. Ding, M. J. Zuo, and A. Lisnianski, "Fuzzy multi-state systems general definition and performance assessment," *IEEE Trans. Rel.*, vol. 57, no. 4, pp. 589–594, Dec. 2008.
- [37] Z. Zhao, Q. Quan, and K.-Y. Cai, "A health monitoring method for Li-ion batteries based on profust Reliability Theory," *Chem. Eng. Trans.*, vol. 33, pp. 961–966, 2013.
- [38] B. Saha and K. Goebel, NASA Ames, Moffett Field, CA, "Battery data set," *NASA Ames Prognostics Data Repository 2007* [Online]. Available: <http://ti.arc.nasa.gov/project/prognostic-data-repository>
- [39] A. Saxena, J. Celaya, B. Saha, S. Saha, and K. Goebel, "Metrics for off-line evaluation of prognostic performance," *Int. J. Prognostics Health Management*, 2010.
- [40] D. Dubois, H. Prade, and C. Testemale, "Weighted fuzzy pattern matching," *Fuzzy Sets Syst.*, vol. 28, no. 3, pp. 313–331, 1988.
- [41] G. Grimmett and D. Stirzaker, *Probability Random Processes*, 3rd ed. Oxford: Clarendon Press, 2001.
- [42] A. Chen and G. S. Wu, "Real-time health prognosis and dynamic preventive maintenance policy for equipment under aging Markovian deterioration," *Int. J. Production Res.*, vol. 45, no. 15, pp. 3351–3379, 2007.
- [43] E. Zio and F. D. Maio, "A data-driven fuzzy approach for predicting the remaining useful life in dynamic failure scenarios of a nuclear system," *Rel. Eng. Syst. Safety*, vol. 95, no. 1, pp. 49–57, 2010.
- [44] A. Saxena, J. Celaya, E. Balaban, K. Goebel, B. Saha, S. Saha, and M. Schwabacher, "Metrics for evaluating performance of prognostics techniques," in *Proc. Int. Conf. Prognostics Health Management*, 2008, pp. 1–17.

Zhiyao Zhao received his B.S. degree in automation from Beijing Technology and Business University, Beijing, China, in 2011. Since 2011, he has been studying in the School of Automation Science and Electrical Engineering, Beihang University (Beijing University of Aeronautics and Astronautics), Beijing, China, pursuing his Ph.D. degree. His current research interest is the area of reliability analysis, and prognostics and health management.

Quan Quan received the B.S., and Ph.D. degrees from Beihang University (Beijing University of Aeronautics and Astronautics), Beijing, China, in 2004, and 2010, respectively. He has been an Associate Professor with Beihang University since 2013, where he is currently with the School of Automation Science and Electrical Engineering. His research interest covers reliable flight control, vision-based navigation, repetitive learning control, and time-delay systems.

Kai-Yuan Cai received the B.S., M.S., and Ph.D. degrees from Beihang University (Beijing University of Aeronautics and Astronautics), Beijing, China, in 1984, 1987, and 1991, respectively. He is a Cheung Kong Scholar (Chair Professor) jointly appointed by the Ministry of Education of China and the Li Ka Shing Foundation of Hong Kong in 1999. He has been a Full Professor with Beihang University since 1995, where he is currently with the School of Automation Science and Electrical Engineering. His main research interests include software reliability and testing, reliable flight control, and software cybernetics. He is a member of the Editorial Board of Fuzzy Sets and Systems, and was the Editor of The Kluwer International Series on Asian Studies in Computer and Information Science. He also was a Guest Editor for Fuzzy Sets and Systems (1996), the International Journal of Software Engineering and Knowledge Engineering (2006), the Journal of Systems and Software (2006), and IEEE TRANSACTIONS ON RELIABILITY (2011).